Synthetic negative feedback circuits using engineered small RNAs

Ciarán L. Kelly[1]*, Andreas W. K. Harris[2], Harrison Steel[2], Edward J. Hancock[2], John T. Heap[1], Antonis Papachristodoulou[2]*

[1] Centre for Synthetic Biology and Innovation, Department of Life Sciences, Imperial College London, South Kensington Campus, London SW7 2AZ, U.K.

[2] Department of Engineering Science, University of Oxford, Parks Road, Oxford OX1 3PJ, U.K.

[3] School of Mathematics and Statistics and Charles Perkins Centre, University of Sydney, Sydney, NSW 2006, Australia

The authors wish it to be known that, in their opinion, the first two authors should be regarded as joint First Authors.

* To whom correspondence should be addressed. Tel: +44 1865283036; Email: antonis@eng.ox.ac.uk. Correspondence may also be addressed to email: ciaran.kelly@imperial.ac.uk or ciaranlk@gmail.com.

ABSTRACT

Negative feedback control is known to endow natural biological and man-made technological systems with robust performance in the face of uncertainties. To date synthetic biological feedback circuits have predominantly relied upon transcription factors and suffer from limitations such as excessive burden and lack of flexible tunability. Small RNAs (sRNAs) are non-coding RNA molecules which can post-transcriptionally regulate gene expression through interaction with messenger RNA (mRNA). In this paper, we present the design, modelling and construction of two new negative feedback architectures that use rationally-designed, translation-inhibiting sRNA modules for the first time. The first circuit builds upon the well characterised *tet*-based autorepressor, allowing fine tuning of the circuit output through the use of an external input molecule that modulates sRNA expression. The second circuit involves an sRNA in direct negative feedback with the output protein of the circuit, regulating the mRNA encoding this protein in response to output protein concentration. Stochastic and deterministic modelling guided the design and optimal implementations of both circuits, and the experimental data obtained compared well with model predictions. The detailed and well-characterised circuits presented in this work can be integrated into larger, more complex, synthetic biological circuits, pathways and systems.

INTRODUCTION

Natural biological systems function through the accurate and reliable control of expression of a large number of genes interacting with each other in response to a variety of environmental or internal signals. The ability to engineer biological systems to perform such complex tasks is a key goal of the field of synthetic biology (1), but with limited success to date (2, 3). Engineering elements and

approaches such as modularity (4), standardisation (5–8), as well as design and analysis frameworks from control engineering (9–11) are becoming widely accepted in synthetic biology practice, yet challenges remain. Modularity in particular has faced many challenges, as many parts do not behave orthogonally or reliably in novel genetic and host contexts (2, 12, 13), resulting in inconsistent performance and even total failure.

Employing feedback mechanisms in synthetic biological circuits can provide robustness and predictability when environmental and genetic contexts change (2, 14, 15). Feedback is ubiquitous in natural biological systems, involved in regulating everything from the production of individual amino acids (16) and nutrients (17, 18); to the levels of transcription factors (19); and even regulating the responses of complex biological systems such as chemotaxis (20), the scaling of morphogen gradients during development (21), and the progress of the entire cell cycle (22–24). Feedback has been employed in many synthetic gene circuits *in vivo*, including circuits such as the toggle switch (25), the repressillator (26), sustained and tunable oscillators (27) and a concentration tracker (28). *In silico* feedback has also been successfully employed to control gene expression (29), with improved understanding leading to more successful synthetic feedback circuits (30).

One commonly-found motif that uses negative feedback is the autorepressor or autoregulator (19, 31–34). This architecture consists of a transcription factor which represses expression of its own encoding gene, by binding to operator sites located in the promoter immediately upstream. As the concentration of the transcription factor increases, its transcription is reduced, thus autoregulating its steady state. This mechanism is found in the regulation of 40% of the known transcription factors of *Escherichia coli* controlling a wide range of cellular processes (19). Autorepression is also crucial to the regulation of virulence factors and the control of quorum signalling in important human pathogens, such as *Vibrio cholerae* (35–37). Synthetic and re-engineered autorepressors based on the *tet* repressor protein, TetR, and its cognate *tet* promoter, P_{tet}, have been constructed and studied in detail to understand their performance and properties such as noise and response kinetics (19, 31, 32). Autorepressor feedback motifs have been shown to reduce the rise time (19), which is the time it takes the circuit to move from 10 % to 90 % of the steady state of the output. This reduction can be advantageous in certain situations where a quick response is crucial.

The use of an autorepressor in synthetic biology is however hindered by the steep, sigmoidally-shaped input-output curve, as tuning the regulated output level using an external input is difficult. For example, in the case of the P_{tet}-TetR autorepressor, the addition of the inducer anhydrotetracycline (aTc) allows only coarse tuning of the output in the steep region of the curve. One way to attempt to overcome this problem could be to re-engineer the feedback strength. This can be achieved through: protein engineering of the transcription factor to alter its interactions with inducer and promoter; mutagenesis of the promoter itself to change transcription-initiation rates; or increasing the low rate of degradation of the species involved in regulation (38, 39), which would reduce the concentration of the repressor in the system, thereby changing the output, and would likely reduce the response time

as this is closely tied to the half-lives of the species involved. However there are two major drawbacks to these solutions. Firstly all three of these solutions are hard-wired into the circuit from the start and therefore cannot be easily manipulated during the course of an experiment. Secondly increasing turnover of proteins will increase burden on the cellular machinery, which can result in undesirable effects such as impaired cell growth. It would therefore be beneficial if alternative negative feedback solutions that bypassed these issues could be integrated into synthetic feedback circuits.

Post-transcriptional control of an output is an appealing route to solving the drawbacks associated with autorepressor-based negative feedback circuits. There has been a resurgence of interest in RNAs as a means of regulation (40, 41), in large part due to a vastly increased understanding of the role of natural regulatory RNAs, but also due to the predictability of the folding and interactions of RNA structures (40). Natural RNA regulators perform a broad range of functions (42, 43), and harnessing these in synthetic circuits could offer a wide range of benefits. Functional RNAs are faster for a host cell to produce and being short RNA strands require less energy than protein production (35), therefore constituting a lower burden to the host, a key consideration for synthetic biological circuits (12). They also have the potential to propagate signals rapidly (44), as their dynamics are tied to the naturally high degradation rate of RNA. In excess of 80 sRNAs have been characterised in *E. coli* alone (42). Hfq (host factor for RNA phage Q beta replication)-associated sRNAs are one class of non protein-coding small RNAs found in many prokaryotes that can bind and regulate mRNA molecules and are of interest to explore in synthetic negative feedback circuits (45, 46). These sRNAs are involved in a wide range of host cellular functions (42, 43, 47–49) and have been studied extensively at the biochemical level (43, 50–53). The regulation of translation by sRNAs can occur through one of four mechanisms: inhibition of translation; activation of translation; stabilisation of the duplexed mRNA; or stimulating degradation of the target mRNA (42, 43, 47, 54). The inhibition of mRNA translation is the most commonly observed sRNA regulation mechanism and is potentially important for the purposes of synthetic negative feedback circuits. The mechanism by which this occurs is through sRNA binding upstream of, or at the 5' end of the open reading frame, thus occluding the ribosome from binding to the ribosome-binding site (RBS) sequence and/or recognising the start codon of the target mRNA. In this manner translation-inhibiting sRNAs operate as summing junctions, reducing the net concentration of mRNA available for translation.

The use of synthetic sRNAs to inhibit translation of a small number of mRNA targets has been reported (13, 55, 56). Models of the inhibition mechanism have been studied (57–59) and verified through comparison with experimental data (60–63). However, due to their high degradation rates, sRNAs are often noisier than their protein-based counterparts (58). Additionally, off-target effects can interfere with endogenous systems in the cell (56) and must be taken into account when designing their use in a particular host organism (64). Despite this, with careful *in silico* design, it is clear that sRNAs offer a powerful alternative feedback mechanism to use in synthetic negative feedback circuits. As synthetic sRNAs operate primarily through complementarity, they can be designed to

target any sequence, allowing the predictable engineering of a much greater number of feedback circuits than currently possible using transcription factors alone.

In this work we have designed, modelled, built and tested two novel synthetic biological negative feedback circuits incorporating Hfq-associated sRNAs. The first circuit combines the well-studied TetR-P_{tet} autorepressor and a translation-inhibiting sRNA, whose expression can be externally tuned, resulting in the introduction of an sRNA-tetR mRNA summing junction into the circuit, allowing fine tuning of the mRNA levels of the repressor TetR in conjunction with the coarse aTc dial. The second circuit consists of an activating transcription factor, RhaS, coupled with negative feedback supplied by translation-inhibiting sRNA. Deterministic and stochastic modelling of both systems was performed to guide design and predict circuit characteristics. Two plasmid and one plasmid implementations of both of these circuits were realised and data from these implementations used to improve the accuracy of the simulations. This work is the first successful use of sRNAs in synthetic biological feedback circuits; it adds an important new tool for designing feedback circuits in cells, which can aid in the design of robust and intricate circuits for future synthetic biology applications.

MATERIALS AND METHODS

Mathematical modelling

Deterministic systems of ordinary differential equations (ODEs) describing the genetic circuits were constructed using standard methods (65, 66). They included a mechanistic model of the interaction between the transcription factor-fusion protein (TetR-sfGFP or RhaS-sfGFP in our case), the promoter (P*tet* or P*rhaBAD*) and the inducer (anhydrotetracycline (aTc) or L-rhamnose), using similar methods described previously (67). The sRNA mechanism was modelled by treating the binding of the target mRNA by the sRNA as irreversible, as previously described (58–60, 62, 63), allowing the concentration of the heteroduplex between the sRNA and target mRNA to be ignored. As superfolder GFP is used, degradation is assumed to be zero and therefore the only factor removing protein from the system is assumed to be dilution by cell growth. This gives protein a half-life equivalent to the doubling time of the host cell (68). mRNA is actively degraded with a half-life of approximately three minutes (69). The half-life of the sRNA in the deterministic case is set to be the same as the protein, as sRNAs have been shown to be protected by the Hfq chaperone proteins (70).

The steady states of the deterministic models were numerically calculated using the MATLAB function ‘fsolve’.

The mechanisms included in the deterministic model were included in the stochastic model as well. A number of additions were made to the stochastic model to more accurately model the experimental set-up as well as the inhibition mechanism. The first addition takes the interaction with the Hfq chaperone protein into account. The way in which this mechanism is modelled is similar to that previously described (57), and takes all forward and reverse interactions between Hfq and the RNA

species (sRNA and target mRNA) into account. The second approach takes the experimental set-up into account, modelling genetic noise and the number of plasmids that are present. It is assumed that plasmids are diluted in a similar manner to proteins and have a half-life equal to the doubling time of the host cell. The production rate is fixed such that the average number of plasmids in the cell is equal to the copy number of the plasmid being modelled.

The stochastic models employed the Gillespie algorithm (71), the models were defined in the Synthetic Biology Mark-up Language (8) and the ensemble simulations of 10000 runs were executed using CudaSim (72). Each individual simulation was run until algorithm time surpassed 300 minutes, at which point it was assumed that the behaviour amounted to fluctuations around the steady state. Only the endpoint of each simulation was used in the analysis. The mean and standard deviation were calculated from the first and second moments and the coefficient of variation is defined to be the standard deviation divided by the mean for a given time point.

Both the stochastic and deterministic equations and parameters, used are presented in Supplementary Information.

Bacterial Strains and Growth Conditions

E. coli strain DH5α was used for all plasmid construction and propagation. Wild-type *E. coli* strain MG1655 was used for initial experiments with pCK200 - pCK209 plasmids. Subsequently the Keio collection *rhaS* mutant JW3876 was used for all further time course assays. Cells were cultured in LB, M9 minimal media supplemented with 0.5 % v/v glycerol or EZ rich defined media (Teknova Inc) supplemented with 0.5 % v/v glycerol at 37 °C. Ampicillin and chloramphenicol were used at final concentrations of 125 µg/mL and 25 µg/mL respectively.

Plasmid Construction

A table of plasmids and oligonucleotides used in this study is provided in Table S7. Sequences of all plasmids have been submitted to EMBL. The Gibson assembly method was used for all assemblies (73) and where DNA was removed, blunt-end cloning of phosphorylated PCR products. All synthetic DNA fragments (gblocks) were synthesised by Integrated DNA Technologies Inc. To construct the initial autorepressor plasmid, pCK200, oligonucleotides oligoCK89 and oligoCK90 were used to amplify the pCK301 backbone and a synthetic gene fragment - containing the tet promoter, a synthetic RBS with a translation initiation rate of 50,000 (designed using Salis RBS calculator (74)) and the *tetR* gene - inserted. To construct the *rhaS*-containing version of the autorepressor plasmid, pCK210, oligonucleotides oligoCK173 and oligoCK174 were used to amplify the *rhaS* RBS and gene from *E. coli* strain MG1655; oligonucleotides oligoCK171 and oligoCK172 were used to amplify the pCK200 backbone and the two fragments combined.

To construct the sRNA-expressing plasmid pCK201, a synthetic sRNA gene fragment was designed based on the pWAS plasmid (55). The probable Shine Dalgarno sequence of the synthetic RBS of the

tetR mRNA was identified (AGTAGGT) and the reverse complement of the 24 nucleotides from the start of this sequence used as the anti-tetR mRNA targeting sequence (TAATCTGGACATTCTGAACCTACT). This sequence was analysed for off target binding using IntaRNA (75) and placed immediately upstream of the Hfq-binding scaffold of the micC sRNA from *E. coli*, followed by the T1/TE transcriptional terminator resulting in the final sRNA-expressing DNA fragment. Finally both the *proD* promoter (76) and λ pR promoters (77) were inserted upstream of this sRNA-encoding sequence and the entire double promoter-sRNA-scaffold construct was synthesised. This synthetic gene fragment was inserted into the backbone of the pSUtat-Sh-GX-EF plasmid, which was linearised using oligonucleotides, oligoCK87 and oligoCK88. The alternative anti-tetR mRNA sRNA plasmid, pCK202, was designed similarly, but the 24 antisense nucleotides chosen to bind to start codon of the tetR mRNA. This targeting sequence was analysed for off target binding, combined with same promoters and scaffold sequences, synthesised and inserted into the same location of pSUtat-Sh-GX-EF backbone. To remove the *proD* promoter, pCK201 was amplified using oligonucleotides, oligoCK121 and oligoCK120 and the resulting PCR fragment ligated by blunt-end cloning, resulting in plasmid pCK208. To remove the pR promoter, pCK201 was amplified using oligonucleotides, oligoCK127 and oligoCK124 and the resulting PCR fragment ligated similarly, resulting in plasmid pCK209.

To construct the *rhaS*-expressing plasmid pAH12, the *proD* promoter from pCK201 was amplified using oligonucleotides, oligoAH003 and oligoAH005, the *rhaS* RBS and gene was amplified from pCK210 using oligonucleotides, oligoAH004 and oligoAH006, and both were inserted into the same backbone PCR product as used for pCK200 construction. To construct the anti-rhaS mRNA sRNA plasmids pAH15 and pAH16, oligonucleotides oligoAH001 and oligoCK88 were used to amplify the backbone of pCK208 and a synthetic gene fragment encoding an sRNA targeting a 24 base pair region of the rhaS mRNA beginning with the start codon in the case of pAH15 and the Shine Dalgarno sequence in the case of pAH16 of the rhaS mRNA, was designed, synthesised and inserted into this backbone fragment. These were analysed for off target binding, and contain the same Hfq-binding and terminator scaffold sequences as in pCK201. pAH17 was constructed using oligonucleotides oligoAH001 and oligoAH013 to amplify the *rhaBAD* promoter from pAH16 and oligoAH12 and oligoAH040 to amplify the sRNA-encoding sequences and backbone of pCK201, which were then assembled to form the finished plasmid. The combined target and sRNA plasmid for sRNA circuit II, pCK218 was constructed as follows. Oligonucleotides oligoCK449 and oligoCK104 were used to amplify the backbone of pAH12 and oligoCK451 and oligoCK450 used to amplify the promoter-sRNA-scaffold sequence from pAH16, and the resulting PCR products combined.

The combined target and sRNA plasmid for the circuit including the autorepressor with the inhibiting sRNA (sRNA circuit 1), pCK215 was constructed as follows. Oligonucleotides oligoCK449 and oligoCK104 were used to amplify the backbone of pCK210 and oligonucleotides oligoCK451 and oligoCK450 used to amplify the *rhaBAD* promoter-sRNA-scaffold sequence from pAH17. The resulting PCR products were combined, resulting in the intermediate plasmid pCK214. Finally in order

to remove excess cargo and reduce the overall size of the composite plasmid, the *lacI* gene was deleted using oligoCK324 and oligoCK100 and the resulting PCR product recircularised using blunt-end ligation yielding the final plasmid pCK215.

Finally, the control plasmid, pAH23 was constructed by removing the section containing the promoters, sRNA and terminator from pCK201 through amplification of the backbone into two fragments using oligonucleotides: oligoAH007 and oligoAH008; and oligoAH009 and oligoAH010., which were subsequently combined resulting in the final plasmid.

Assays

E. coli MG1655 or JW3876 (Δ*rhaS* Keio collection mutant) cells were transformed with appropriate plasmid(s) and isolated transformants used to inoculate 5 ml of EZ rich defined media (rich media hereafter) or M9 minimal media (minimal media hereafter) supplemented with 0.5 % (v/v) glycerol, as appropriate, and ampicillin or chloramphenicol, which was cultured with shaking at 37 °C for 16 h. For the high resolution flow cytometry experiments, these cultures were then subcultured into 300 µL of fresh media in deep 96 well plates, to an optical density (OD; A600 nm) of 0.05 and the plate incubated at 37 °C with rapid shaking. For circuits using the *tet* promoter, the tetracycline analogue, anhydrotetracycline (aTc) was added to the assay cultures at the concentrations specified. For circuits using the *rhaBAD* promoter for expression, the inducer L-rhamnose was added to the assay cultures at the concentrations specified. Samples were taken at specific time points for optical density and GFP fluorescence measurements. A FLUOstar Omega platereader (BMG Labtech) was used for all absorbance measurements of optical density (OD) at A600 nm and GFP fluorescence measured using an Attune NXT flow cytometer (ThermoFisher Scientific). Cells were gated using forward and side scatter, and GFP fluorescence (excitation and emission wavelengths: 488 and 525 nm [with 20 nm bandwidth] respectively) was measured. Histograms of fluorescence intensity were plotted, and mean and coefficient of variations statistics extracted. For the lower resolution platereader experiments, overnight cultures were subcultured into 150 µL of fresh media in 96-well microplates, to an optical density (OD; A600 nm) of 0.05 and the plate incubated at 37 °C with rapid shaking in a FLUOstar Omega platereader (BMG Labtech). Optical density and GFP fluorescence (excitation and emission wavelengths: 485 and 530 nm [with 20 nm bandwidth] respectively) were measured every 15 minutes, with fluorescence normalised by optical density and plotted over time.

RESULTS

Model-based feedback design with sRNA

The architectures of the three circuits we set out to design, model, build and test are shown in Figure 1. Our starting point was the autorepressor (Figure 1A), with an external inducer (u_1) that can be used to regulate the level of output protein. The second circuit introduces a synthetic sRNA, which is used to regulate the amount of mRNA subsequently translated into the repressor protein (Figure 1B). The inclusion of the translation-inhibiting sRNA gives a means of interfering with the negative feedback

loop through a second external inducer (u_2), allowing the concentration of the repressor protein to be regulated. Intuitively, a higher level of sRNA expression leads to lower concentrations of repressor. With the effective feedback strength of the autorepressor being reduced, one would expect a longer rise time. At the same time, the inclusion of the sRNA may come at a cost to noise in some operating regimes, and therefore it is important to determine whether there is a trade-off between the strength of the feedback and the noise level that can be achieved.

The third circuit consists of an sRNA module in feedback with a transcriptional module (Figure 1C). In this circuit, expression of the translation-inhibiting sRNA is activated by a transcriptional activator in response to an external input (u_3). The activator itself is constitutively expressed and its mRNA is the target of the translation-inhibiting sRNA. This is a very interesting circuit due to its unique architecture in that the sRNA module is in a closed feedback loop with the transcriptionally-activating module. We want to explore how the steady state level of activator for this circuit responds when the level of the inducer is increased, but also what the noise properties of this feedback are.

The following sections present the experimental implementations of these circuits. Before embarking on experiments, we also modelled the various architectures, which revealed beneficial properties that were subsequently used to guide the construction of each of the circuits. We used deterministic modelling to predict the mean behaviour of a given circuit across a population, but cells are stochastic, noisy, time varying systems; heterogeneity is always present across a population. Noise comes from two sources: intrinsic and extrinsic. Extrinsic noise stems from changes to environment or variations in the amount of general cellular machinery available. Intrinsic noise is due to the stochastic nature of biochemical reactions. We modelled transcription, translation and degradation of all species; the sRNA inhibition mechanism is modelled as an irreversible association of the target mRNA and sRNA (58–60, 62, 63). The activation and inhibition mechanisms are modelled explicitly or using Hill functions depending on the context. More details of the specific models used are given in the associated Supplementary Information.

A translation-inhibiting sRNA regulates the effective feedback strength of the autorepressor

Design and validation of an autorepressor

An autorepressor based on the *tet*-repressor mechanism (19, 31–34) was constructed. The circuit consists of the *tet* promoter, P_{tet}, which controls the transcription of a gene encoding a TetR-superfolder green fluorescent protein (sfGFP) fusion protein, which allows convenient and quantitative monitoring of the output via fluorescence. A synthetic ribosome-binding site (RBS) was designed with a translation initiation rate (T.I.R.) of 50,000 (74) and inserted upstream of this open reading frame. This expression unit was then inserted into the backbone of the medium copy (pBR322 replicon; 15-20 copies per cell) *E. coli* expression plasmid pCK301 (78), resulting in pCK200 (Figure S7A), and the qualitative performance of the circuit tested. The *E. coli* strain MG1655 was transformed with pCK200, cultured in minimal media over 24 hours, with samples taken at regular timepoints and analysed by

flow cytometry (Figure S7B). The behaviour of the circuit is in good agreement with previously described autoregulatory circuits (32), with the characteristic sharp levelling off of fluorescence over time (Figure S7B). Next the behaviour of the autorepressor circuit was investigated using an external input (u_1). The experiment was repeated with the addition of three concentrations of the inducer anhydrotetracycline (aTc), fluorescence and optical density measured after 6 h and normalised fluorescence plotted (Figure 2A). As previously shown, aTc increased the maximum fluorescence level reached before autorepression re-establishes, thus allowing an external input with which to set the output level of the system. Dose responses of the mean output and the coefficients of variation with increasing concentrations of aTc, during exponential growth in rich media are in good agreement with the reference circuit (Figure S7E&F) and predictive modelling results (Figure S7C&D). The starting point for our second negative feedback circuit was thus considered validated.

Designing an sRNA for the autorepressor

Having established the autorepressor component, we next set about integrating a translation-inhibiting small RNA (sRNA) into this circuit. The Hfq-binding scaffold of the *E. coli* micC sRNA and the strong Rho-independent T1/TE terminator were chosen, based on the design principles of previously described synthetic sRNAs (55, 56, 77). In order to maximize translation inhibition of the target tetR-sfGFP mRNA, two different targeting sequences, each 24 nucleotides in length, were designed and tested. The first sequence was designed to bind the first 24 nucleotides of the tetR-sfGFP open reading frame (named “Start” hereafter) and the second designed to bind 24 nucleotides including all of the probable Shine Dalgarno sequence upstream of the tetR-sfGFP open reading frame (named “SD” hereafter). Both sequences were computationally analysed for the strength of binding to the tetR-sfGFP mRNA and for off-target binding to the wild-type *E. coli* (MG1655) ribonucleome using IntaRNA, the most sensitive RNA-RNA interaction software available (75, 79, 80). Binding of the SD sRNA to the tetR-sfGFP mRNA (-37.35 kcal/mol) was more energetically favourable than that of the Start sRNA and tetR-sfGFP mRNA pair (-31.09 kcal/mol), implying stronger binding. Both of these sRNA constructs were inserted into the backbone of the low copy (p15A replicon, 15-20 copies per cell) *E. coli* expression plasmid, pSUtat-GX-EF (a derivative of pSU40) (81, 82). Next a number of different promoters were used to test the translation-inhibiting performance of each of the two sRNAs: Start; and SD. Firstly, the strong constitutive *proD* promoter (P_{proD}) and the lambda pR promoter (P_{pR}), were inserted in tandem upstream of either the SD sRNA construct (pCK201) or the Start sRNA construct (pCK202). Two promoters were inserted in series to allow future reduction of the transcription rate through simple removal of either promoter. To test the performance of these sRNA constructs, *E. coli* strain MG1655 was transformed with pCK200 and either pCK201, pCK202 or pAH23 (empty vector control; no sRNA) and grown in minimal media with different concentrations of aTc in a microplate reader, with fluorescence and optical density (OD_{600nm}) measured after 6h and normalised fluorescence plotted(Figure 2A). The SD-targeting sRNA (pCK201) is clearly better than the Start-targeting sRNA (pCK202) at inhibiting translation of the tetR-sfGFP mRNA, even in the presence of a large concentration of aTc (100 ng/ml). Therefore, the SD-targeting sRNA was taken forward for all subsequent experiments in this circuit.

Introducing the external input to control sRNA levels

Using the SD sRNA construct, we next explored how tunable the sRNA inhibition of translation was. We made two further modifications to pCK201 to reduce expression of the sRNA, removing each of the two constitutive promoters separately, leaving only the lambda pR promoter (pCK208) or the *proD* promoter (pCK209). A modified version of the tetR-sfGFP autorepressor plasmid pCK200 was constructed to use with the sRNA plasmids, whereby the *E. coli rhaS* gene, encoding the transcriptional activator of the *E. coli rhaBAD* promoter (required in later implementation of the sRNA-autorepressor circuit), was inserted downstream of *ampR*, resulting in pCK210, which performed similarly to pCK200 (Figure S12). To test the effect of reduced sRNA transcription on the TetR-sfGFP output, *E. coli* strain MG1655 was transformed with pCK210 and one of pCK201, pCK209 or pAH23, cultured in rich media with increasing concentrations of aTc and analysed by flow cytometry after 4 h. Encouragingly, the level of sRNA inhibition observed in cells containing pCK209 was intermediate, between cells lacking sRNA, pAH23, and cells containing the double promoter sRNA construct, pCK201 (Figure 2B), confirming that the steady state level of the output could be set by altering the expression level of the sRNA. This ability to set the output did not correspond to large changes in the noise profile of the circuit, as the response of the coefficient of variation, a relative measure of the noise about the mean, to increasing concentrations of aTc is similar in all three sample groups (Figure 2C). However, constitutive promoters are static and therefore to allow a second external input to the system, the inducible *rhaBAD* promoter from *E. coli* (P_{rhaBAD}) was inserted in place of the constitutive promoters, resulting in pAH17. This promoter was chosen as it has a predictable and linear dose response to inducer; is tightly off in the absence of inducer; and a non-metabolisable, non-toxic inducer is now available (78). This now enables control over a second input to the system. To validate this inducible sRNA plasmid, *E. coli* strain JW3876, lacking *rhaS*, was transformed with both pCK210 and pAH17, cultured in rich media to mid-exponential phase (4 h) and fluorescence analysed by flow cytometry (Figure 2D). As expected the addition of the inducer L-rhamnose led to inhibition of translation, with a drop in mean fluorescence of between 0 and 0.4 mg/ml of inducer. This result confirmed that we could alter the amount of sRNA in a cell by varying the concentration of L-rhamnose, which allows us to tune the negative feedback of the autorepressor through a second external input (u_2 in Figure 1B) in later experiments.

Finally, to lower the potential cellular burden of maintaining two plasmids in the host organism and to proactively counter any effect of having the two halves of the circuit on two separate plasmids introduce excess noise into the system, the inducible sRNA and autorepressor constructs were combined onto one plasmid, pCK215 (Figure 3A) and the behaviour of this circuit was in good agreement with the two plasmid system (pCK210 + pAH17) (Figure S12B).

Modelling and testing of the autorepressor circuit containing the translation-inhibiting sRNA.

The experimental results were next compared with the ordinary differential equations and stochastic models described (SI Section 2). A surface plot showing the expected steady state concentration of TetR-sfGFP, referred to as the output, is presented in Figure S4. In our experiments, the fluorescence

intensity of TetR-sfGFP is used as a proxy for protein concentration. The dose response of this circuit to aTc is similar to that of the simple autorepressor. The addition of the sRNA provides a second means of controlling the output. The saturated level of expression of TetR-sfGFP is capped by the expression of sRNA: a higher level of sRNA expression results in a lower saturated level.

Two experiments to test the model were designed. First, the concentration of the inducer aTc is varied but the transcription rate of the sRNA is fixed. This is equivalent to the use of pAH17 and one concentration of L-rhamnose; alternatively, one of the constitutively-expressing sRNA plasmids, pCK201 or pCK209 can be used. Our model predicted that interfering with the negative feedback of the autorepressor would result in an increase in the steady state until saturation occurs (Figure S8A). A prediction of the coefficients of variation in response to interference in negative feedback through increasing concentrations of aTc, was also performed. This predicted a drop in noise as the circuit is induced, prior to levelling off (Figure S8B).

The second experiment fixed the concentration of aTc, while varying the expression rate of the sRNA, through the use of the plasmid pCK215 (autorepressor and inducible sRNA) and increasing concentrations of the second inducer L-rhamnose. Our model predicted that the steady state would decrease, as expected, as sRNA levels increase (Figure 3B) until a threshold is reached, where the concentration of sRNA is so high that hardly any TetR-sfGFP mRNA is translated. This threshold concentration of sRNA corresponds to an increase in noise (coefficient of variation) (Figure 3C). The combination of deterministic and stochastic modelling therefore, shows that the two input dials can be used simultaneously to control the steady state output of the system and the corresponding noise behaviour predicted.

Using these predictions, we tested our circuits to see how they perform relative to the stochastic modelling. As the steady state of the output is not reached before stationary phase in this experimental set up and as stationary phase of bacterial cultures is almost impossible to model with confidence, an assessment of the biological circuits in relation to the deterministic modelling was not attempted. Flow cytometry was used throughout as it measures the fluorescence intensity of each individual cell allowing stochastic statistics of a population to be measured. *E. coli* strain JW3876 was transformed with pCK215 and grown in rich media with different concentrations of aTc and fluorescence measured after 4 h (Figure S8C). The observed response of mean fluorescence to aTc concentration was in good agreement with the computationally-predicted results (Figure S8A). The shape of the response of the coefficient of variation to increasing aTc concentrations (Figure S8D) is also in good agreement with the prediction (Figure S8B).

Finally this circuit was tested by fixing the concentration of aTc at a moderate concentration of 40 ng/ml and varying the concentration of the second inducer, L-rhamnose, resulting in increased transcription of the sRNA and ultimately higher cellular concentrations of sRNA. Similar experiments were performed with *E. coli* strain JW3876 transformed with pCK215 in rich media and varying

concentrations of L-rhamnose. Mean fluorescence decreases between 0 and 0.4 mg/ml L-rhamnose and then levels off (Figure 3D), matching the trend seen in the model (Figure 3B), albeit at a higher output level than the model predicted. The coefficient of variation was lower at low concentrations of L-rhamnose, with a small increase at high concentrations (Figure 3E), which was similar to the behaviour predicted, if less severe.

A translation-inhibiting sRNA dynamically responds in closed-loop to increased protein levels by regulating the protein-coding mRNA.

Design and construction of the closed-loop feedback circuit

We wanted to explore alternative feedback circuits where sRNAs could be used to great effect. The circuit which we set out to design and implement is shown schematically in Figure 1C, whereby an activating transcription factor when supplied with an external input (u_3) induces expression of a translation-inhibiting sRNA, which itself targets the mRNA of the activator, thus forming a closed loop with its transcription. Circuits with this architecture are found in nature, suggesting an evolutionary fitness for this motif (83).

To construct this circuit, the *E. coli rhaS* gene encoding the transcriptional activator of the rhamnose catabolism operon, RhaS, was inserted into the *E. coli* expression vector pCK301 (78), resulting in a translational fusion of RhaS to sfGFP (RhaS-sfGFP hereafter). The strong constitutive *proD* promoter was inserted upstream of *rhaS*, resulting in the plasmid pAH12. As previously performed, two sRNAs were designed, one which would target the Shine Dalgarno of the rhaS mRNA and another that would target the start codon of the rhaS mRNA. sRNA-mRNA binding strengths and off target effects were analysed using IntaRNA, with the SD sRNA found to bind more favourably than the Start sRNA to the rhaS-sfGFP mRNA (-36.01 kcal/mol versus -33.53 kcal/mol respectively). Each sRNA was inserted onto the same low copy vector as in the previous circuit (pSUtat-Sh-GX-EF). To complete the RhaS-sRNA feedback loop, the *E. coli* rhamnose promoter (P_{rhaBAD}) was placed upstream of each sRNA unit, resulting in the finished plasmids pAH15 (Start) and pAH16 (SD), allowing expression of the sRNA in the presence of both RhaS and L-rhamnose or its non-metabolisable analogue, L-mannose (78). To validate that this circuit was functional, *E. coli* strain JW3876 was transformed with pAH12 and either pAH15 (Start) or pAH16 (SD) and transformants cultured in minimal media with varying concentrations of L-rhamnose in a microplate reader. Fluorescence and optical density (OD_{600nm}) were measured after 6 h and normalised fluorescence plotted (Figure S9). Encouragingly even at a low concentration of L-rhamnose (0.2 mg/ml), both sRNAs are capable of reducing the level of RhaS-sfGFP production. The SD-targeting version was found to inhibit rhaS-sfGFP mRNA translation more effectively than the Start-targeting version (Figure S9) and used for the final single-plasmid circuit.

The *rhaS-sfGFP* expression unit and the inducible SD-targeting sRNA unit were subsequently combined on one plasmid and validated (data not shown), resulting in pCK218 (Figure 4A). Both the two plasmid and one plasmid circuit architectures were investigated using stochastic modelling and the high resolution flow cytometry experiments.

Modelling and testing of the closed-loop feedback circuit

We constructed and analysed a deterministic and a stochastic model of this circuit, as before. The steady state of the output of the system, the concentration of RhaS-sfGFP, was first explored using deterministic modelling. The surface plot in Figure S5 represents the dose response. As the concentration of L-rhamnose increases, the steady state is predicted to decrease, as one would expect. In addition to this, changing the rate of transcription of the *rhaS-sfGFP* is also modelled. If the rate of transcription of the *rhaS-sfGFP* is higher than the maximum rate of expression of the sRNA, there will always be a measurable output (Figure S5). The model predicts that if the rate of transcription of *rhaS-sfGFP* is lower than the maximal rate of sRNA expression, then the system has an 'off' state. As the implementation used here drives the expression of *rhaS-sfGFP* using a strong constitutive promoter, P_{proD}, the system operates in the former regime where the maximal rate of expression of sRNA is lower than the transcription rate of *rhaS-sfGFP*, so no 'off' state should exist.

The stochastic model was used to predict the variability in a population of cells containing this circuit. The relative strengths of the transcription rates of the sRNA and the target *rhaS-sfGFP* mRNA informs the choice of parameters for the stochastic simulations. Using the single-plasmid system, pCK218, we modelled the effect of increasing numbers of sRNA molecules on the mean RhaS-sfGFP protein output per cell (Figure 4B). As expected, mean protein output decreases rapidly as the concentration of L-rhamnose increases, corresponding to an increase in the number of sRNA molecules in the cell. The coefficient of variation remains fairly constant across the range of L-rhamnose concentrations modelled (Figure 4C).

With the information from the deterministic and stochastic modelling in mind, experiments were designed and performed to measure the response of the mean fluorescence intensity of each cell to increasing L-rhamnose concentrations. *E. coli* strain JW3876 was transformed with pCK218 and transformants cultured in rich media with various concentrations of L-rhamnose, and fluorescence measured by flow cytometry after 4 h. The initial range of inducer concentrations of 0 to 4 mg/ml did not allow for high-resolution analysis of the concentration response, implying that the induction of the circuit is shifted towards very low concentrations of L-rhamnose. The second lower range of inducer concentrations of 0, 0.001, 0.005 and 0.1 mg/ml L-rhamnose allowed the concentration response of both mean fluorescence intensity and the coefficient of variation to be observed. In good agreement with the predicted response, mean fluorescence drops rapidly between 0 and 0.001 mg/ml L-rhamnose and remains constant at higher concentrations (Figure 4D). The coefficients of variation, although higher than predicted, remain within 0.2 across all concentrations of L-rhamnose tested, decreasing slightly with increasing L-rhamnose (Figure 4E).

We noticed that the population histograms for the one plasmid system have a narrow main peak but small broad shoulders on either side, resulting in the higher than expected coefficients of variation (Figure S10). Further gating of events to this main central peak (>90% of cells) reduces the variation

around the mean at all L-rhamnose concentrations, with a tight showing a tight distribution around the mean.

Comparison of one versus two plasmid implementations of sRNA circuits

In the course of this work, we noticed interesting differences in the predicted noise profiles of each sRNA circuit with respect to whether the DNA sequences encoding it was located either entirely on the chromosome, entirely on a single plasmid or split across two plasmids. With the first sRNA circuit, where the negative feedback of the autorepressor is reduced using the translation-inhibiting sRNA, the predicted coefficients of variation differ widely when modelled with a circuit on either the chromosome, one plasmid or split across two plasmids. With the chromosomal/singular plasmid implementations, the coefficient of variation increases with increasing L-rhamnose concentrations before levelling off at 1 mg/ml of L-rhamnose (Figure 5A). With the two plasmid implementation however, the coefficient of variation starts to rise at low concentrations of L-rhamnose and increases rapidly (Figure 5A). The implications of this are that it will be almost impossible to tune the level of the output species (RhaS-sfGFP) without excessive noise. This trend was observed with experiments conducted with either pCK215 alone or the combination of pCK210 and pAH17 plasmids (Figure 8B). These differences were not observed in the predicted or experimentally-derived dose response of mean protein output (Figure S11A).

Similarly the chromosomal, single plasmid and two plasmid implementations of the second closed-loop sRNA circuit, where the sRNA represses the translation of the mRNA encoding the activator required for its own transcription also showed stark differences. In this case noise increased with each move of the system from chromosome to single plasmid and then to the two plasmid system (Figure 5C). The difference between one and two plasmid implementations was even greater in the experimental data, where the coefficient of variation jumps to greater than 20 for the two plasmid (pAH12 and pAH16) versus the one plasmid system (pCK218) which remains constant throughout, as predicted by the modelling. In fact three distinct modal populations of cells were observed during flow cytometry of cultures of cells containing the two plasmids (Figure S13). Differences in means were almost indistinguishable across the chromosomal/one/two plasmid implementations (Figure S11B). Clearly this level of noise is unacceptable for any application of these feedback circuits.

DISCUSSION

In this paper we have described for the first time, the design, modelling, construction, testing and improvement of two synthetic feedback circuits using translation-inhibiting small RNAs. The first sRNA circuit introduced an sRNA-mRNA summing junction into the TetR autorepressor feedback loop, which reduces the amount of tetR mRNA translated. We have shown that the level of sRNA expression can be set, through the use of constitutive promoters of different strengths or inducible promoters, and that the designed circuit behaves as expected, with a reduction in the circuit output with increasing sRNA expression. In the case of the L-rhamnose inducible sRNA module, this provides an additional, external input (other than aTc) with which to change the output levels of the

feedback circuit; one that is faster acting than the transcription factor-based module, highlighting a key advantage of the use of sRNAs over proteins in feedback circuits. If operated in a regime of relatively high aTc levels and intermediate levels of sRNA expression, the system exhibits a linear response at no cost to noise levels, in contrast to the sigmoidal response with aTc alone.

In the second sRNA circuit we built a closed-loop feedback circuit consisting of an sRNA that responds to the level of the circuit output protein, in this case the transcriptional activator RhaS, by regulating the level of translation of the mRNA encoding the output. The inducer in this circuit, L-rhamnose, binds with the output protein and this transcription factor-inducer complex regulates the level of sRNA transcription, thus closing the loop. We have shown that the addition of the external input and subsequent increase in sRNA expression, correlates as expected with a reduction in output protein levels. The predicted noise profile for this circuit is level at a constant coefficient of variation of just below 0.2, which is the same as in the case of the autorepressor. The experimentally-derived noise profile for the circuit was higher, yet decreased slightly with increasing concentrations of L-rhamnose. This feedback circuit provides a very robust expression of the output protein and is likely to have very good disturbance rejection properties, where the steady-state protein concentration remains constant with environmental or other changes, as output level plateaus at a certain input concentration and does not fluctuate at higher concentrations. The rapid dynamics of direct sRNA negative feedback contribute to this robust disturbance rejection property, whereby changes in the production of RhaS through modifying its rate of mRNA translation are not affected by changes in the L-rhamnose concentration above a nominal level.

In addition to the above, the mathematical models predicted a number of features that were not explicitly observed, but to a large extent led to interest in the circuits prior to implementation. The first such prediction relates to the rise times of the studied circuits. The rise time of the autorepressor is well studied (19), and was therefore used as a baseline of comparison for the two circuits presented in this paper. Deterministic simulation of these circuits predict that the autorepressor with an sRNA responds 20% slower than the plain autorepressor, whereas the circuit where the loop is closed through the inhibiting sRNA responds twice as fast as the autorepressor (Figure S6), strengthening the hypothesis that this is in large part be due to the rapid dynamics associated with sRNAs themselves.

Our mathematical models, gave very good predictions of the measured responses. In particular, we have demonstrated good correlation of the coefficient of variation between experiments and stochastic modelling that matched the expected behaviour of the circuits. This was more evident when we considered splitting the circuit across two plasmids, where we have seen noise levels increasing. This underlines the fact that the precise implementation of a circuit design is key, and mathematical modelling can help in the choice in this case.

Although there is good qualitative agreement between the modelled coefficient of variation and the experimental data, the absolute values are different, with the experimental values being consistently higher that the modelled values. This is likely due to the stochastic simulations only accounting for intrinsic noise, i.e. the noise caused by the interactions directly modelled and not extrinsic noise, such as environmental fluctuations or functions of the cell such as replication and division (84, 85)), whereas the experimental data account for both intrinsic and extrinsic noise. This was most evident in the second sRNA circuit, where a small population of cells (< 10 %) displayed highly variable mean outputs, a result that was not predicted by modelling. L-Rhamnose consumption by *E. coli* is unlikely to be the cause of this variation as almost identical results were obtained using the non-metabolisable analogue inducer of the system, L-mannose (data not shown), and similarly bimodality in populations of cells from the *rhaBAD* promoter has not been seen to date (78). It would be interesting to see if altering the level of *rhaS* transcription through the use of a different inducible promoter in place of P_{proD}, affected the noise profile and indeed overall performance of this circuit. Additionally it should be noted that estimating parameters for models involving transcription factors such as RhaS is extremely difficult, as biochemical characterisation (structural, kinetics) of these proteins itself is challenging: proteins containing largely unstructured DNA-binding domains are recalcitrant to purification. One possible solution to this uncertainty with transcription factor behaviour could be to try a number of different inducible promoter systems in parallel, such as the XylS-Pm system from *Pseudomonas putida*, which responds to m-toluic acid (86).

Another interesting difference between predicted and experimentally-observed output of the first sRNA circuit was the ability to reach lower output levels when the sRNA was expressed using strong constitutive promoters than when using the inducible *rhaBAD* promoter and high concentrations of L-rhamnose. As P_{rhaBAD} is capable of high levels of transcription, this observation is unlikely to result from differences in expression strengths from each promoter. An alternative explanation, especially since we are observing the circuits during their transient response, could be that using an inducible promoter introduces a delay in the transcription of the sRNA compared to constitutive promoters, and this delay may enable the autorepressor to complete its negative feedback circuit faster than sRNA production, thus the output level remains higher than when this delay is absent when constitutive promoters are used.

In this paper we have also learned important information regarding the design of synthetic sRNAs for use in synthetic biology circuits. We have found that using synthetic sRNAs that cover all of the RBS of the mRNA they are targeting performed better than those targeting the start codon of the mRNA. On the one hand this contradicts the strong guidelines outline by other groups previously (55), which advises start codon targeting over SD targeting. However our data is in good agreement with another finding in the same paper, showing that the free energy of sRNA-mRNA binding should be below the threshold of approximately -36 kcal/mol where inhibition of translation is 99% effective. We conclude therefore that designing a synthetic sRNA with binding energies below this threshold is of greater importance than whether the sRNA targets the RBS or start codon.

While the designs are very simple and use well-characterised, commonly-employed components, their interconnection in a feedback fashion demonstrates the advantages of different architectures, as predicted by mathematical modelling. Although the output of both feedback circuits outlined in this paper was a transcription factor fused to a fluorescent reporter protein, this could easily be modified to include almost any other single protein of interest. One could imagine modified versions of the circuit being used to regulate and optimise the commercial production of protein therapeutics and industrially-relevant enzymes, as well as in metabolic engineering where the stoichiometry of pathway enzymes must be tightly controlled. The use of a non-protein component in a negative feedback circuit such as this, may also aid these applications through the expected reduction in cellular burden associated with using an sRNAs over another resource-sapping protein. And finally, as sRNAs are simple nucleotide oligomers, with careful design they can be constructed to target almost any mRNA sequence required, a feat that is impossible with transcription factors. Indeed one sRNA sequence can be designed to target multiple mRNAs with different efficiencies, opening up the possibility of synthetic genetic feedback circuits of greater complexity than has been possible to date.

ACCESSION NUMBERS

ENA study accession number: PRJEB87181

SUPPLEMENTARY DATA

Supplementary Data are available at NAR online.

ACKNOWLEDGEMENTS

The authors thank Dr. George Wadhams and Prof. Judith Armitage for their support and advice.

FUNDING

This work was supported by the Biotechnology and Biological Sciences Research Council [BB/M011321/1 to J.T.H.] and the Engineering and Physical Sciences Research Council [EP/M002454/1 to A.P.]. Funding for open access charges: Engineering and Physical Sciences Research Council.

CONFLICT OF INTEREST

The authors declare no competing financial interest.

TABLE AND FIGURE LEGENDS

Figure 1. Schematic diagrams of the circuits investigated in this study. A. Autorepressor. B. sRNA Circuit I consisting of an autorepressor and a translation-inhibiting sRNA, which regulates the translation of the autorepressor mRNA. C. sRNA Circuit II consisting of a transcriptional activator in

closed-loop feedback with a translation-inhibiting sRNA.

Figure 2. Testing of sRNA designs and analysis of the effect of different promoters on function. A. Plasmids encoding sRNAs targeting the Shine Dalgarno (pCK201) or start codon (pCK202) were designed. *E. coli* MG1655 cells were transformed with one of these plasmids and pCK200 (Autorepressor) and the ability of each sRNA construct to inhibit translation of the tetR-sfGFP mRNA with increasing concentrations of aTc assessed by monitoring fluorescence. B. *E. coli* JW3876 cells were transformed with pCK210 (a derivative of pCK200; *rhaS* added downstream of *ampR*) and one of pAH23 (no sRNA), pCK201 (two constitutive promoters, Pr and PproD, upstream of sRNA), or pCK209 (PproD promoter only upstream of sRNA), cultured in EZ rich defined medium and fluorescence measured with increasing concentrations of aTc. C. The coefficient of variation about the mean tetR-sfGFP fluorescence from *E. coli* JW3876 cells with pCK210 and pAH23, pCK201 or pCK209 with increasing concentrations of aTc. D. *E. coli* JW3876 cells were transformed with pCK210 and pAH17 (PrhaBAD promoter upstream of sRNA), cultured in EZ rich defined medium with increasing concentrations of L-rhamnose to mid-exponential phase and the fluorescence measured.

Figure 3. Layout and comparison of predicted versus experimentally-measured output of pCK215 (autorepressor plus inducible sRNA on one plasmid) with increasing concentrations of L-rhamnose with fixed concentration of aTc (40 ng/ml). A. Architecture of the sRNA circuit I plasmid, pCK215 combining the autorepressor with translation-inhibiting sRNA on one plasmid. B. Predicted dose response of the output of sRNA circuit I to increasing concentrations of L-rhamnose. C. Predicted response of the coefficient of variation of the output of sRNA circuit I to increasing concentrations of L-rhamnose. D. Experimentally measured dose response of mean TetR-sfGFP fluorescence of *E. coli* JW3876 cells transformed with pCK215, grown in EZ rich defined medium to mid-exponential phase with a fixed concentration of aTc (40 ng/ml) and increasing concentrations of L-rhamnose. E. Experimentally measured response of the coefficient of variation of mean TetR-sfGFP fluorescence from *E. coli* JW3876 cells transformed with pCK215, with a fixed concentration of aTc (40 ng/ml) and increasing concentrations of L-rhamnose.

Figure 4. Layout and comparison of predicted versus experimentally-measured output of pCK218 (RhaS transcriptional activator in closed loop feedback with inducible sRNA on one plasmid) with increasing concentrations of L-rhamnose. A. Architecture of the sRNA circuit II plasmid, pCK218 encoding the transcriptional activator RhaS and the translation-inhibiting sRNA on one plasmid. B. Predicted dose response of the output of sRNA circuit II to increasing concentrations of L-rhamnose. C. Predicted response of the coefficient of variation of the output of sRNA circuit II to increasing concentrations of L-rhamnose. D. Experimentally measured dose response of mean TetR-sfGFP fluorescence of *E. coli* JW3876 cells transformed with pCK218, grown in EZ rich defined medium to mid-exponential phase with increasing concentrations of L-rhamnose. E. Experimentally measured response of the coefficient of variation of mean TetR-sfGFP fluorescence from *E. coli* JW3876 cells transformed with pCK218, with increasing concentrations of L-rhamnose.

Figure 5. The effect of splitting components of both sRNA circuits across different plasmids. A & C Predictive modelling of the coefficient of variation with respect to increasing concentrations of L-rhamnose. B & D Experimental data of the response of the coefficient of variation of the mean with increasing concentrations of L-rhamnose.

REFERENCES

1. Andrianantoandro,E., Basu,S., Karig,D.K. and Weiss,R. (2006) Synthetic biology: new engineering rules for an emerging discipline. *Mol. Syst. Biol.*, **2**, 2006.0028.

2. Anderson,J., Strelkowa,N., Stan,G.-B., Douglas,T., Savulescu,J., Barahona,M. and Papachristodoulou,A. (2012) Engineering and ethical perspectives in synthetic biology. Rigorous, robust and predictable designs, public engagement and a modern ethical framework are vital to the continued success of synthetic biology. *EMBO Rep.*, **13**, 584–590.

3. Kwok,R. (2010) Five hard truths for synthetic biology. *Nature*, **463**, 288–290.

4. Del Vecchio,D. (2015) Modularity, context-dependence, and insulation in engineered biological circuits. *Trends Biotechnol.*, **33**, 111–119.

5. Müller,K.M. and Arndt,K.M. (2012) Standardization in synthetic biology. *Methods Mol. Biol.*, **813**, 23–43.

6. Canton,B., Labno,A. and Endy,D. (2008) Refinement and standardization of synthetic biological parts and devices. *Nat. Biotechnol.*, **26**, 787–793.

7. Arkin,A. (2008) Setting the standard in synthetic biology. *Nat. Biotechnol.*, **26**, 771–774.

8. Hucka,M., Finney,A., Sauro,H.M., Bolouri,H., Doyle,J.C., Kitano,H., Arkin,A.P., Bornstein,B.J., Bray,D., Cornish-Bowden,A., *et al.* (2003) The systems biology markup language (SBML): a medium for representation and exchange of biochemical network models. *Bioinformatics*, **19**, 524–531.

9. Oishi,K. and Klavins,E. (2011) Biomolecular implementation of linear I/O systems. *IET Syst. Biol.*, **5**, 252–260.

10. Chen,Y.-J., Dalchau,N., Srinivas,N., Phillips,A., Cardelli,L., Soloveichik,D. and Seelig,G. (2013) Programmable chemical controllers made from DNA. *Nat. Nanotechnol.*, **8**, 755–762.

11. Harris,A.W.K., Dolan,J.A., Kelly,C.L., Anderson,J. and Papachristodoulou,A. (2015) Designing Genetic Feedback Controllers.

12. Borkowski,O., Ceroni,F., Stan,G.-B. and Ellis,T. (2016) Overloaded and stressed: whole-cell considerations for bacterial synthetic biology. *Curr. Opin. Microbiol.*, **33**, 123–130.

13. Ceroni,F., Furini,S., Stefan,A., Hochkoeppler,A. and Giordano,E. (2012) A Synthetic Post-transcriptional Controller To Explore the Modular Design of Gene Circuits. *ACS Synth. Biol.*, **1**, 163–171.

14. Afroz,T. and Beisel,C.L. (2013) Understanding and exploiting feedback in synthetic biology. *Chem. Eng. Sci.*, **103**, 79–90.

15. Khammash,M. (2016) An engineering viewpoint on biological robustness. *BMC Biol.*, **14**, 22.

16. Hoffmann,B., Valerius,O., Andermann,M. and Braus,G.H. (2001) Transcriptional autoregulation and inhibition of mRNA translation of amino acid regulator gene cpcA of filamentous fungus Aspergillus nidulans. *Mol. Biol. Cell*, **12**, 2846–2857.

17. El-Samad,H., Goff,J.P. and Khammash,M. (2002) Calcium homeostasis and parturient hypocalcemia: an integral feedback perspective. *J. Theor. Biol.*, **214**, 17–29.

18. Yang,X.-W., He,Y., Xu,J., Xiao,X. and Wang,F.-P. (2013) The Regulatory Role of Ferric Uptake Regulator (Fur) during Anaerobic Respiration of Shewanella piezotolerans WP3. *PLoS One*, **8**, e75588.

19. Rosenfeld,N., Elowitz,M.B. and Alon,U. (2002) Negative autoregulation speeds the response times of transcription networks. *J. Mol. Biol.*, **323**, 785–793.

20. Alon,U., Surette,M.G., Barkai,N. and Leibler,S. (1999) Robustness in bacterial chemotaxis. *Nature*, **397**, 168–171.

21. Ben-Zvi,D. and Barkai,N. (2010) Scaling of morphogen gradients by an expansion-repression integral feedback control. *Proceedings of the National Academy of Sciences*, **107**, 6924–6929.

22. Sheldrick,K.S. and Carr,A.M. (1993) Feedback controls and G2 checkpoints: fission yeast as a model system. *Bioessays*, **15**, 775–782.

23. Murakami,H. and Nurse,P. (2000) DNA replication and damage checkpoints and meiotic cell cycle controls in the fission and budding yeasts. *Biochem. J*, **349**, 1–12.

24. Dasso,M. and Newport,J.W. (1990) Completion of DNA replication is monitored by a feedback system that controls the initiation of mitosis in vitro: Studies in Xenopus. *Cell*, **61**, 811–823.

25. Gardner,T.S., Cantor,C.R. and Collins,J.J. (2000) Construction of a genetic toggle switch in Escherichia coli. *Nature*, **403**, 339–342.

26. Elowitz,M.B. and Leibler,S. (2000) A synthetic oscillatory network of transcriptional regulators. *Nature*, **403**, 335–338.

27. Stricker,J., Cookson,S., Bennett,M.R., Mather,W.H., Tsimring,L.S. and Hasty,J. (2008) A fast, robust and tunable synthetic gene oscillator. *Nature*, **456**, 516–519.

28. Hsiao,V., de Los Santos,E.L.C., Whitaker,W.R., Dueber,J.E. and Murray,R.M. (2014) Design and Implementation of a Biomolecular Concentration Tracker. *ACS Synth. Biol.*, 10.1021/sb500024b.

29. Milias-Argeitis,A., Rullan,M., Aoki,S.K., Buchmann,P. and Khammash,M. (2016) Automated optogenetic feedback control for precise and robust regulation of gene expression and cell growth. *Nat. Commun.*, **7**, ncomms12546.

30. Potvin-Trottier,L., Lord,N.D., Vinnicombe,G. and Paulsson,J. (2016) Synchronous long-term oscillations in a synthetic gene circuit. *Nature*, **538**, 514–517.

31. Becskei,A. and Serrano,L. (2000) Engineering stability in gene networks by autoregulation. *Nature*, **405**, 590–593.

32. Dublanche,Y., Michalodimitrakis,K., Kummerer,N., Foglierini,M. and Serrano,L. (2006) Noise in transcription negative feedback loops: simulation and experimental analysis. *Mol.Syst.Biol.*, **2**, 41.

33. Austin,D.W., Allen,M.S., McCollum,J.M., Dar,R.D., Wilgus,J.R., Sayler,G.S., Samatova,N.F., Cox,C.D. and Simpson,M.L. (2006) Gene network shaping of inherent noise spectra. *Nature*, **439**, 608–611.

34. Nevozhay,D., Adams,R.M., Murphy,K.F., Josić,K. and Balázsi,G. (2009) Negative autoregulation linearizes the dose–response and suppresses the heterogeneity of gene expression. *Proceedings of the National Academy of Sciences*, **106**, 5123–5128.

35. Svenningsen,S.L., Waters,C.M. and Bassler,B.L. (2008) A negative feedback loop involving small RNAs accelerates Vibrio cholerae's transition out of quorum-sensing mode. *Genes Dev.*, **22**, 226–238.

36. Holmqvist,E., Unoson,C., Reimegård,J. and Wagner,E.G.H. (2012) A mixed double negative

feedback loop between the sRNA MicF and the global regulator Lrp. *Mol. Microbiol.*, **84**, 414–427.

37. Nitzan,M., Shimoni,Y., Rosolio,O., Margalit,H. and Biham,O. (2015) Stochastic analysis of bistability in coherent mixed feedback loops combining transcriptional and posttranscriptional regulations. *Phys. Rev. E Stat. Nonlin. Soft Matter Phys.*, **91**, 052706.

38. Koch,A.L. and Levy,H.R. (1955) Protein turnover in growing cultures of Escherichia coli. *J. Biol. Chem.*, **217**, 947–957.

39. Nath,A. and Koch,A.L. (1970) Protein Degradation in Escherichia coli. MEASUREMENT OF RAPIDLY AND SLOWLY DECAYING COMPONENTS. *Journal of Biological Chemistry*, **245**, 2899–2900.

40. Peters,G., Coussement,P., Maertens,J., Lammertyn,J. and De Mey,M. (2015) Putting RNA to work: Translating RNA fundamentals into biotechnological engineering practice. *Biotechnol. Adv.*, **33**, 1829–1844.

41. Chappell,J., Watters,K.E., Takahashi,M.K. and Lucks,J.B. (2015) A renaissance in RNA synthetic biology: new mechanisms, applications and tools for the future. *Curr. Opin. Chem. Biol.*, **28**, 47–56.

42. Waters,L.S. and Storz,G. (2009) Regulatory RNAs in bacteria. *Cell*, **136**, 615–628.

43. Gottesman,S. (2005) Micros for microbes: non-coding regulatory RNAs in bacteria. *Trends Genet.*, **21**, 399–404.

44. Takahashi,M.K., Chappell,J., Hayes,C.A., Sun,Z.Z., Kim,J., Singhal,V., Spring,K.J., Al-Khabouri,S., Fall,C.P., Noireaux,V., *et al.* (2015) Rapidly Characterizing the Fast Dynamics of RNA Genetic Circuitry with Cell-Free Transcription–Translation (TX-TL) Systems. *ACS Synth. Biol.*, **4**, 503–515.

45. Modi,S.R. and Camacho,D.M. (2011) Functional characterization of bacterial sRNAs using a network biology approach. *Proceedings of the …*, **108**.

46. Storz,G., Vogel,J. and Wassarman,K.M. (2011) Regulation by small RNAs in bacteria: expanding frontiers. *Mol. Cell*, **43**, 880–891.

47. Opdyke,J.A., Kang,J.-G. and Storz,G. (2004) GadY, a Small-RNA Regulator of Acid Response Genes in Escherichia coli. *J. Bacteriol.*, **186**, 6698–6705.

48. Guisbert,E., Rhodius,V.A., Ahuja,N., Witkin,E. and Gross,C.A. (2007) Hfq modulates the sigmaE-mediated envelope stress response and the sigma32-mediated cytoplasmic stress response in Escherichia coli. *J. Bacteriol.*, **189**, 1963–1973.

49. Massé,E., Salvail,H., Desnoyers,G. and Arguin,M. (2007) Small RNAs controlling iron metabolism. *Curr. Opin. Microbiol.*, **10**, 140–145.

50. Tomizawa,J., Itoh,T., Selzer,G. and Som,T. (1981) Inhibition of ColE1 RNA primer formation by a plasmid-specified small RNA. *Proc. Natl. Acad. Sci. U. S. A.*, **78**, 1421–1425.

51. Stougaard,P., Molin,S. and Nordström,K. (1981) RNAs involved in copy-number control and incompatibility of plasmid R1. *Proc. Natl. Acad. Sci. U. S. A.*, **78**, 6008–6012.

52. Altuvia,S., Weinstein-Fischer,D., Zhang,A., Postow,L. and Storz,G. (1997) A small, stable RNA induced by oxidative stress: role as a pleiotropic regulator and antimutator. *Cell*, **90**, 43–53.

53. Majdalani,N., Cunning,C., Sledjeski,D., Elliott,T. and Gottesman,S. (1998) DsrA RNA regulates translation of RpoS message by an anti-antisense mechanism, independent of its action as an antisilencer of transcription. *Proc. Natl. Acad. Sci. U. S. A.*, **95**, 12462–12467.

54. Storz,G., Opdyke,J.A. and Zhang,A. (2004) Controlling mRNA stability and translation with small, noncoding RNAs. *Curr. Opin. Microbiol.*, **7**, 140–144.

55. Na,D., Yoo,S.M., Chung,H., Park,H., Park,J.H. and Lee,S.Y. (2013) Metabolic engineering of Escherichia coli using synthetic small regulatory RNAs. *Nat. Biotechnol.*, **31**, 170–174.

56. Man,S., Cheng,R., Miao,C., Gong,Q., Gu,Y., Lu,X., Han,F. and Yu,W. (2011) Artificial trans-encoded small non-coding RNAs specifically silence the selected gene expression in bacteria. *Nucleic Acids Res.*, **39**, e50.

57. Adamson,D.N. and Lim,H.N. (2011) Essential Requirements for Robust Signaling in Hfq Dependent Small RNA Networks. *PLoS Comput. Biol.*, **7**, e1002138.

58. Mehta,P., Goyal,S. and Wingreen,N.S. (2008) A quantitative comparison of sRNA-based and protein-based gene regulation. *Mol. Syst. Biol.*, **4**, 221.

59. Shimoni,Y., Friedlander,G., Hetzroni,G., Niv,G., Altuvia,S., Biham,O. and Margalit,H. (2007) Regulation of gene expression by small non-coding RNAs: a quantitative view. *Mol. Syst. Biol.*, **3**, 138.

60. Hussein,R. and Lim,H.N. (2012) Direct comparison of small RNA and transcription factor signaling. *Nucleic Acids Res.*, **40**, 7269–7279.

61. Sagawa,S., Shin,J.-E., Hussein,R. and Lim,H.N. (2015) Paradoxical suppression of small RNA activity at high Hfq concentrations due to random-order binding. *Nucleic Acids Res.*, **43**, 8502–8515.

62. Levine,E., Zhang,Z., Kuhlman,T. and Hwa,T. (2007) Quantitative Characteristics of Gene Regulation by Small RNA. *PLoS Biol.*, **5**, e229.

63. Legewie,S., Dienst,D., Wilde,A., Herzel,H. and Axmann,I.M. (2008) Small RNAs establish delays and temporal thresholds in gene expression. *Biophys. J.*, **95**, 3232–3238.

64. Kery,M.B., Feldman,M., Livny,J. and Tjaden,B. (2014) TargetRNA2: identifying targets of small regulatory RNAs in bacteria. *Nucleic Acids Res.*

65. Ingalls,B. (2013) Mathematical modelling in systems biology: An introduction. *Internet. [cited at p. 117]*.

66. Alon,U. (2006) An Introduction to Systems Biology: Design Principles of Biological Circuits CRC Press.

67. Hancock,E.J., Stan,G.-B., Arpino,J.A.J. and Papachristodoulou,A. (2015) Simplified mechanistic models of gene regulation for analysis and design. *J. R. Soc. Interface*, **12**, 20150312.

68. Maurizi,M.R. (1992) Proteases and protein degradation inEscherichia coli. *Experientia*, **48**, 178–201.

69. Granger,L.L., O'Hara,E.B., Wang,R.F., Meffen,F.V., Armstrong,K., Yancey,S.D., Babitzke,P. and Kushner,S.R. (1998) The Escherichia coli mrsC gene is required for cell growth and mRNA decay. *J. Bacteriol.*, **180**, 1920–1928.

70. Saramago,M., Bárria,C., Dos Santos,R.F., Silva,I.J., Pobre,V., Domingues,S., Andrade,J.M., Viegas,S.C. and Arraiano,C.M. (2014) The role of RNases in the regulation of small RNAs. *Curr. Opin. Microbiol.*, **18C**, 105–115.

71. Gillespie,D.T. (1976) A general method for numerically simulating the stochastic time evolution of coupled chemical reactions. *J. Comput. Phys.*, **22**, 403–434.

72. Zhou,Y., Liepe,J., Sheng,X., Stumpf,M.P.H. and Barnes,C. (2011) GPU accelerated biochemical network simulation. *Bioinformatics*, **27**, 874–876.

73. Gibson,D.G., Young,L. and Chuang,R.Y. (2009) Enzymatic assembly of DNA molecules up to several hundred kilobases. *Nature*, **6**, 12–16.

74. Salis,H.M., Mirsky,E. a. and Voigt,C. a. (2009) Automated design of synthetic ribosome binding

sites to control protein expression. *Nat. Biotechnol.*, **27**, 946–950.

75. Busch,A., Richter,A.S. and Backofen,R. (2008) IntaRNA: efficient prediction of bacterial sRNA targets incorporating target site accessibility and seed regions. *Bioinformatics*, **24**, 2849–2856.

76. Davis,J.H., Rubin,A.J. and Sauer,R.T. (2011) Design, construction and characterization of a set of insulated bacterial promoters. *Nucleic Acids Res.*, **39**, 1131–1141.

77. Yoo,S.M.S.M., Na,D. and Lee,S.Y.S.Y. (2013) Design and use of synthetic regulatory small RNAs to control gene expression in Escherichia coli. *Nat. Protoc.*, **8**, 1694–1707.

78. Kelly,C.L., Liu,Z., Yoshihara,A., Jenkinson,S.F., Wormald,M.R., Otero,J.M., Estévez,A.M., Kato,A., Marqvorsen,M.H.S., Fleet,G.W.J., *et al.* (2016) Synthetic chemical inducers and genetic decoupling enable orthogonal control of the rhaBAD promoter. *ACS Synth. Biol.*

79. Wright,P.R., Georg,J., Mann,M., Sorescu,D.A., Richter,A.S., Lott,S., Kleinkauf,R., Hess,W.R. and Backofen,R. (2014) CopraRNA and IntaRNA: predicting small RNA targets, networks and interaction domains. *Nucleic Acids Res.*, **42**, W119–23.

80. Ying,X., Cao,Y., Wu,J., Liu,Q., Cha,L. and Li,W. (2011) sTarPicker: a method for efficient prediction of bacterial sRNA targets based on a two-step model for hybridization. *PLoS One*, **6**, e22705.

81. Kelly,C.L., Pinske,C., Murphy,B.J., Parkin,A., Armstrong,F., Palmer,T. and Sargent,F. (2015) Integration of an [FeFe]-hydrogenase into the anaerobic metabolism of Escherichia coli. *Biotechnology Reports*, **8**, 94–104.

82. Bartolomé,B., Jubete,Y., Martínez,E. and de la Cruz,F. (1991) Construction and properties of a family of pACYC184-derived cloning vectors compatible with pBR322 and its derivatives. *Gene*, **102**, 75–78.

83. Thompson,K.M., Rhodius,V.A. and Gottesman,S. (2007) σE Regulates and Is Regulated by a Small RNA in Escherichia coli. *J. Bacteriol.*, **189**, 4243–4256.

84. Paulsson,J. (2004) Summing up the noise in gene networks. *Nature*, **427**, 415–418.

85. Elowitz,M.B., Levine,A.J., Siggia,E.D. and Swain,P.S. (2002) Stochastic gene expression in a single cell. *Science*, **297**, 1183–1186.

86. Inouye,S., Nakazawa,A. and Nakazawa,T. (1987) Overproduction of the xylS gene product and activation of the xylDLEGF operon on the TOL plasmid. *J. Bacteriol.*, **169**, 3587–3592.

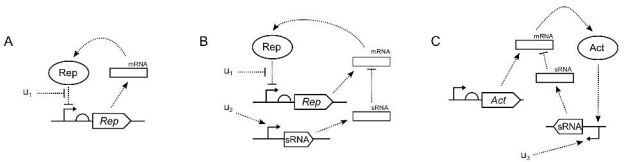
A
Rep
mRNA
u1
Rep
B
Rep
mRNA
u1
Rep
u2
sRNA
sRNA
C
mRNA
Act
sRNA
Act
sRNA
u3

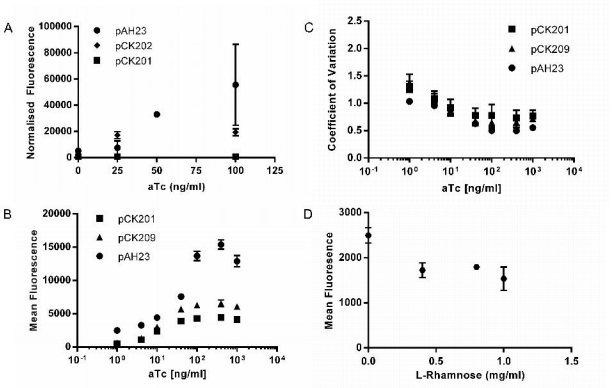
A
Normalised Fluorescence
100000
80000
60000
40000
20000
0
0
25
50
75
100
125
aTc (ng/ml)
pAH23
pCK202
pCK201
B
Mean Fluorescence
20000
15000
10000
5000
0
10^{-1}
10^{0}
10^{1}
10^{2}
10^{3}
10^{4}
aTc [ng/ml]
pCK201
pCK209
pAH23
C
Coefficient of Variation
2.5
2.0
1.5
1.0
0.5
0.0
10^{-1}
10^{0}
10^{1}
10^{2}
10^{3}
10^{4}
aTc [ng/ml]
pCK201
pCK209
pAH23
D
Mean Fluorescence
3000
2000
1000
0
0.0
0.5
1.0
1.5
L-Rhamnose (mg/ml)

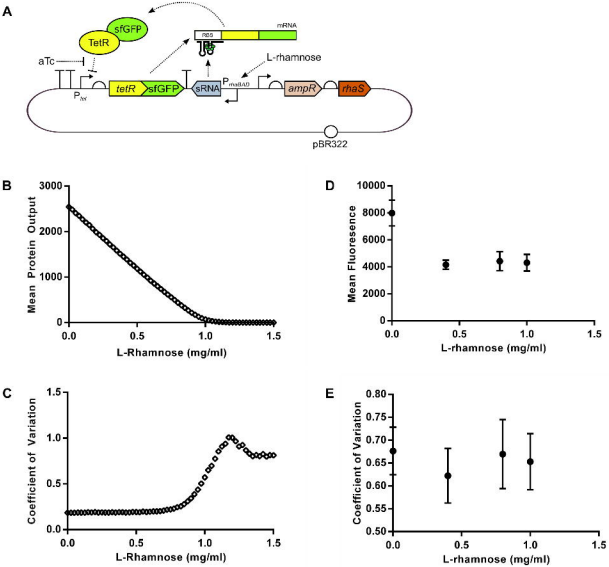
A
sfGFP
TetR
aTc
mRNA
L-rhamnose
tetR
sfGFP
sRNA
ampR
rhaS
pBR322
B
Mean Protein Output
L-Rhamnose (mg/ml)
C
Coefficient of Variation
L-Rhamnose (mg/ml)
D
Mean Fluoresence
L-rhamnose (mg/ml)
E
Coefficient of Variation
L-rhamnose (mg/ml)

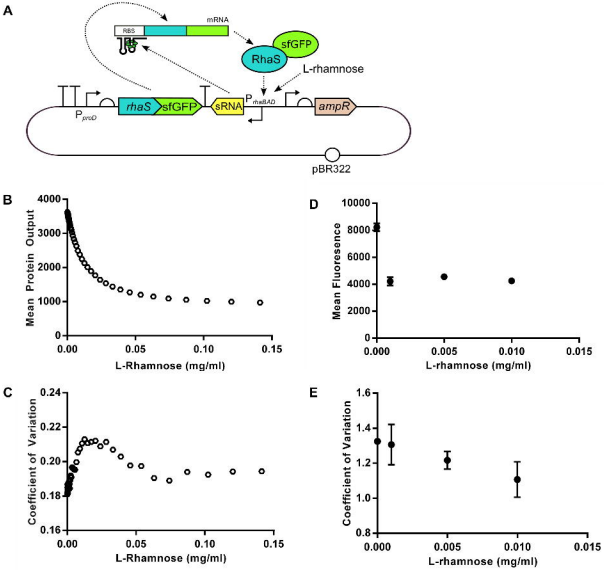
A
mRNA
RBS
sfGFP
RhaS
L-rhamnose
rhaS
sfGFP
sRNA
ampR
pBR322
B
Mean Protein Output
L-Rhamnose (mg/ml)
C
Coefficient of Variation
L-Rhamnose (mg/ml)
D
Mean Fluoresence
L-rhamnose (mg/ml)
E
Coefficient of Variation
L-rhamnose (mg/ml)

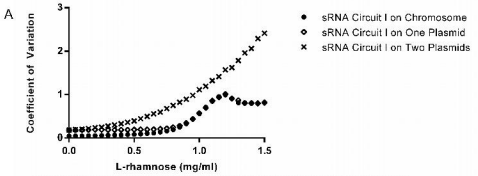
A
Coefficient of Variation
L-rhamnose (mg/ml)
sRNA Circuit I on Chromosome
sRNA Circuit I on One Plasmid
sRNA Circuit I on Two Plasmids

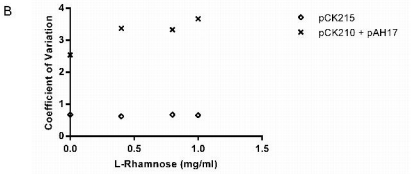
B
Coefficient of Variation
L-Rhamnose (mg/ml)
pCK215
pCK210 + pAH17

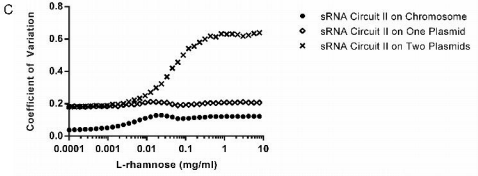
C
Coefficient of Variation
L-rhamnose (mg/ml)
sRNA Circuit II on Chromosome
sRNA Circuit II on One Plasmid
sRNA Circuit II on Two Plasmids

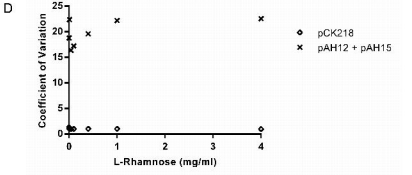
D
Coefficient of Variation
L-Rhamnose (mg/ml)
pCK218
pAH12 + pAH15